Discrete-Time Sliding Mode Spatial Control of Advanced Heavy Water Reactor

Ravindra K. Munje, Balasaheb M. Patre, and Akhilanand P. Tiwari

***Abstract*— This brief presents the design of a discrete-time sliding mode control (DSMC) for spatial power stabilization of advanced heavy water reactor (AHWR). Mathematical model of AHWR is represented by 90 first-order nonlinear differential equations with 18 outputs and five inputs. The linear model is obtained by linearizing nonlinear equations over the rated power. This linear model is found to be highly ill conditioned and is possessing three-time-scale property. Initially, the linear model is transformed into block diagonal form to separate slow, fast 1, and fast 2 subsystems and then DSMC is designed using slow subsystem alone since fast 1 and fast 2 subsystems are stable. The proposed DSMC strategy is designed using the constant plus proportional rate reaching law with matched disturbance. Finally, the nonlinear multivariable model of AHWR is simulated with the designed controller and the results are generated under different transients. The efficacy of the proposed DSMC is demonstrated with the comparison of prevalent controllers in the literature and the performance is evaluated under the same transient levels.**

***Index Terms*— Advanced heavy water reactor (AHWR), composite control, discrete-time sliding mode control (DSMC), global power control in large reactors, reaching law, spatial control.**

I. Introduction

VARIABLE structure control with sliding mode control (SMC) was first proposed and elaborated in the early 1950s in Soviet Union [1], [2]. The discontinuous nature of control action in sliding mode results in robust system performance, which includes insensitivity to parameter variations and complete rejection of disturbance [2]–[4]. Extensive study of discrete-time systems and design of discrete-time SMC (DSMC) has been accelerated due to the use of digital computers and samplers in control realization. The analysis and design of controllers for discrete two-time-scale systems has been studied in [5]–[8]. Block diagonalization of discrete three-time-scale system is also presented in [8] and [9]. Although the system designed with DSMC has number of advantages, the complexity in DSMC design increases with the increase in number of states of the system. Hence, for a higher order ill-conditioned system, the DSMC design is also more complicated. DSMC of singularly perturbed two-time-scale systems has been attempted in [10]–[13].

Recently, a heavy water moderated thermal reactor named as advanced heavy water reactor (AHWR) has been designed in India [14]. This reactor is neutronically large requiring a spatial control system. The AHWR model is highly nonlinear, large scale, heavily ill conditioned, and found to possess three-time-scale property. Hence, model-order reduction and time-scale decomposition methods are generally employed for controller design. Application of DSMC for spatial control of pressurized heavy water reactor (PHWR) can be found in [15] and [16]. In [15] and [16], multirate output feedback (MROF)-based discrete-time sliding mode controllers (DSMCs) are proposed for PHWR. These control methods do not require state information for feedback purposes and hence are easier to implement. For systems exhibiting multi-time-scale property like AHWR, these methods are not easily applicable. In this brief, the design of DSMC for spatial control of AHWR has been successfully applied. The results obtained using the proposed method are compared with other approaches available in the literature and found to give better performance under the same transients. The rest of this brief is organized as follows. In Section II, a brief overview of AHWR is given. Section III presents the DSMC design for three-time-scale system. The application to AHWR and transient simulations are demonstrated in Section IV, followed by the conclusion in Section V.

II. Brief Overview of AHWR

AHWR is a 920 MW (thermal), vertical pressure tube type reactor, cooled by boiling light water and fueled with (Th-^{233}U)O_2 and (Th-Pu)O_2 pins [14]. The AHWR has eight absorber rods, eight shim rods, and eight regulating rods (RRs) as a part of reactivity control devices. The AHWR core has physical dimension much greater than the neutron migration length causing xenon-induced spatial oscillations in power [17]. This necessitates the regulation of global (total) as well as spatial power over time. The AHWR core is divided in 17 relatively large nodes. The following nonlinear equations constitute the mathematical model of AHWR [18]–[20]:

$$\frac{dP_i}{dt} = (\rho_i - \alpha_{ii} - \beta)\frac{P_i}{\ell} + \sum_{j=1}^{17} \alpha_{ji}\frac{P_j}{\ell} + \lambda C_i \quad (1)$$

$$\frac{dC_i}{dt} = \frac{\beta}{\ell}P_i - \lambda C_i \quad (2)$$

$$\frac{dI_i}{dt} = \gamma_I \Sigma_{fi} P_i - \lambda_I I_i \quad (3)$$

$$\frac{dX_i}{dt} = \gamma_X \Sigma_{fi} P_i + \lambda_I I_i - (\lambda_X + \bar{\sigma}_{Xi} P_i) X_i \quad (4)$$

Manuscript received May 20, 2014; revised December 18, 2014 and March 28, 2015; accepted May 3, 2015. Date of publication June 1, 2015; date of current version December 21, 2015. Manuscript received in final form May 10, 2015. This work was supported by the Board of Research in Nuclear Sciences, Department of Atomic Energy, Government of India, under Project 2009/36/102-BRNS. Recommended by Associate Editor A. Zolotas.

R. K. Munje is with the Department of Electrical Engineering, K. K. Wagh Institute of Engineering Education and Research, Nashik 422003, India (e-mail: ravimunje@yahoo.co.in).

B. M. Patre is with the Department of Instrumentation Engineering, Shri Guru Gobind Singhji Institute of Engineering and Technology, Nanded 431606, India (e-mail: bmpatre@ieee.org).

A. P. Tiwari is with the Reactor Control Division, Bhabha Atomic Research Centre, Mumbai 400085, India (e-mail: aptiwari@barc.gov.in).

Color versions of one or more of the figures in this paper are available online at http://ieeexplore.ieee.org.

Digital Object Identifier 10.1109/TCST.2015.2432136

$$\frac{dH_k}{dt} = \kappa \upsilon_k \tag{5}$$

$$e_{\upsilon x_i}\frac{dx_i}{dt} = P_i - q_{d_i}(h_w - h_d) - q_{d_i}x_i h_c \tag{6}$$

$$e_{xh}\frac{dh_d}{dt} = q_f(\hat{k}_2 h_f - \hat{k}_1) - q_d(\hat{k}_2 h_d - \hat{k}_1) \tag{7}$$

where $i = 1, 2, \ldots, 17$ and $k = 2, 4, 6, 8$. α_{ji} and α_{ii} denote the coupling coefficients between jth and ith nodes and self-coupling coefficients of the ith node, respectively. P, C, I, X, and H are the nodal powers, effective one group delayed neutron precursor, iodine and xenon concentrations, and RR positions, respectively. x_i and h_d denote the exit quality and downcomer enthalpy, respectively. Other notations and symbols have their usual meanings. Values of $e_{\upsilon x_i}$ and e_{xh} along with neutronic parameters, nodal volumes, nodal cross sections, nodal powers, coolant flow rates under full power operation, and coupling coefficients are given in [21]. The reactivity term ρ_i in (1) is expressed as $\rho_i = \rho_{i_u} + \rho_{i_X} + \rho_{i_\alpha}$, where ρ_{i_u}, ρ_{i_X}, and ρ_{i_α} are the reactivity feedbacks due to the control rods, xenon, and coolant void fraction, respectively, given by

$$\rho_{i_u} = \begin{cases} (-10.234H_i + 676.203) \times 10^{-6}, & \text{if } i = 2, 4, 6, 8 \\ 0 & \text{elsewhere} \end{cases}$$

$$\rho_{i_X} = -\frac{\bar{\sigma}_{Xi}X_i}{\Sigma_{ai}}$$

$$\rho_{i_\alpha} = -5 \times 10^{-3}(9.2832x_i^5 - 27.7192x_i^4 + 31.7643x_i^3 - 17.7389x_i^2 + 5.2308x_i + 0.0792).$$

Linearizing (1)–(7) around rated values, linear state-space model can be obtained with the state vector defined as

$$\mathbf{z} = \begin{bmatrix} \mathbf{z}_H^T & \mathbf{z}_X^T & \mathbf{z}_I^T & \delta h_d & \mathbf{z}_C^T & \mathbf{z}_x^T & \mathbf{z}_P^T \end{bmatrix}^T \tag{8}$$

where $\mathbf{z}_H = [\delta H_2\ \delta H_4\ \delta H_6\ \delta H_8]^T$ and the rest $\mathbf{z}_\xi = [(\delta\xi_1/\xi_{1_0}), \ldots, (\delta\xi_{17}/\xi_{17_0})]^T$, $\xi = X, I, C, x, P$, in which δ denotes the deviation from the respective steady-state value of the variable. Likewise, define the input vector as

$$\mathbf{u} = [\delta\upsilon_2 \quad \delta\upsilon_4 \quad \delta\upsilon_6 \quad \delta\upsilon_8]^T \tag{9}$$

with υ_k as the voltage signal to kth RR drive and output vector as

$$\mathbf{y} = \begin{bmatrix} y_g & y_1 & \cdots & y_{17} \end{bmatrix}^T \tag{10}$$

where $y_g = \sum_{i=1}^{17}(\delta P_i/\sum_{j=1}^{17} P_{j_0})$ and $y_i = (\delta P_i/P_{i_0})$ correspond to normalized global reactor power and nodal powers, respectively. Then, the system given by (1)–(7) can be expressed in standard linear state-space form as

$$\dot{\mathbf{z}} = \mathbf{A}\mathbf{z} + \mathbf{B}\mathbf{u} + \mathbf{B}_f\delta q_f \tag{11}$$

$$\mathbf{y} = \mathbf{M}\mathbf{z} \tag{12}$$

where q_f is the feed water flow rate. Note that, the AHWR system has five inputs, namely, four voltage signals to RR drives, mentioned in (9), and a feed water flow rate q_f. Feed water flow rate is assumed to be directly proportional to the global reactor power as $q_f = q_{f0}(\sum_{i=1}^{17} P_i/\sum_{i=1}^{17} P_{i0})$, where q_{f0} and P_{i0} are the steady-state values of feed water flow rate and nodal powers, respectively. Matrices $\mathbf{A}$, $\mathbf{B}$, $\mathbf{B}_f$, and $\mathbf{M}$ are given in [21]. Furthermore, it is observed that the eigenvalues of system matrix $\mathbf{A}$ fall in three distinct clusters. First cluster has 38 eigenvalues, ranging from -1.8870×10^{-4} to 7.455×10^{-3}, and is termed as slow subsystem. Second cluster of 35 eigenvalues, that ranges from -1.8395×10^{-1} to -1.2514×10^{-2}, is termed as fast 1 subsystem and the third cluster, indicating fast 2 subsystem, has 17 eigenvalues ranging from -2.7626×10^2 to -7.2516. It can be noted that, the eigenvalues in fast 1 and fast 2 subsystems are in the left half of s-plane. However, the slow subsystem has four eigenvalues at origin along with six eigenvalues with positive real parts, which indicate instability. Hence, it is necessary to design an effective spatial controller for AHWR. This spatial stabilization and control is achieved by proper movement of RRs. Therefore, out of the five inputs, four inputs to RRs [given by (9)] and a feed water flow rate are written separately in (11).

III. Control Problem of AHWR System

AHWR has large physical dimension. Hence, serious situation may arise in which different regions of the core may undergo variations in neutron flux in opposite phases. If these variations and subsequent oscillations in power distribution are not controlled, the power density and the rate of change of power at some locations in the reactor core may exceed their respective thermal limits, resulting into increased chances of fuel failure. Hence, spatial control, i.e., to prevent spatial oscillations from growing, is required. This has been attempted in [21] and [22] using static output feedback. However, static output feedback does not guarantee stability of closed-loop system. Hence, state feedback-based approaches [23], [24] have been applied to AHWR. However, these control strategies require a state observer of large order. To overcome this, MROF-based fast output sampling (FOS) control technique is investigated in [9]. In FOS, control signal is generated as a linear combination of a number of output samples collected in one sampling interval, where input sampling time is larger compared with output. For example, in [9], sampling time for spatial control component of input is taken as 60 s. A similar kind of approach for two-time-scale system is suggested in [25] for AHWR, where the sampling time is taken as 54 s. However, for practical reactor control to work with larger sampling time is not desirable, because in small time, reactor system can undergo a considerable change. Hence, periodic output feedback (POF)-based controller for three-time-scale system of AHWR is presented in [26] with a sampling period of 2 s. Although MROF-based controllers (i.e., FOS and POF) give a very simple control structure, they lack robustness and may not work satisfactorily in the presence of disturbance, parameter variations, and perturbation in operating conditions. Hence, a single-input fuzzy logic controller [27] and robust continuous-time SMC (CSMC) [28] are proposed for spatial control of AHWR. In [28], AHWR system is decoupled into slow and fast subsystems by two-stage decomposition and CSMC is designed using merely slow subsystem states.

The 17 node model of the AHWR, given by the set of (1)–(7) represents the neutronics and thermal hydraulic

behavior of the core reasonably, i.e., there is always some uncertainty in values of coupling coefficients (α_{ji} and α_{ii}) and the coefficients appearing in (6) and (7). Furthermore, the accuracy of the model is better with larger number of nodes in the core. These kinds of situations can be better handled by robust controller, like SMC. For this reason, DSMC is proposed for spatial control of AHWR. The AHWR model is of very high order and numerically ill conditioned, making the control problem difficult to solve. However, the three-time-scale property exhibited by the model can be exploited to simplify the problem. Hence, the higher order system of AHWR is decomposed into three subsystems [8]. Thereafter, DSMC law based on the reaching law approach is designed using slow subsystem alone, such that it should withstand any external disturbance in the input channels without causing much variation in the nodal powers. This controller is applied to the nonlinear system of AHWR and the simulation results are generated. These results are compared with the CSMC technique presented in [28] and DSMC obtained by two-stage decomposition.

IV. Discrete-Time Sliding Mode Control for Three-Time-Scale Systems

Consider a linear time invariant, controllable continuous-time system as

$$\dot{\mathbf{z}}(t) = \mathbf{A}\mathbf{z}(t) + \mathbf{B}\mathbf{u}(t) + \mathbf{D}_c\mathbf{f}(t) \tag{13}$$

$$\mathbf{y}(t) = \mathbf{M}\mathbf{z}(t). \tag{14}$$

Sampling systems (13) and (14) with sampling period τ yields

$$\mathbf{z}_{k+1} = \Phi\mathbf{z}_k + \Gamma\mathbf{u}_k + \mathbf{D}\mathbf{f}_k \tag{15}$$

$$\mathbf{y}_k = \mathbf{M}\mathbf{z}_k \tag{16}$$

where $\mathbf{z} \in \Re^n$ is the state, $\mathbf{u} \in \Re^m$ is the input, $\mathbf{y} \in \Re^p$ is the output, and $\mathbf{f} \in \Re^r$ is the disturbance. The matrices Φ, Γ, $\mathbf{M}$, and $\mathbf{D}$ are of appropriate dimensions. The disturbance part in (15) is considered to be bounded and satisfies the matching condition [29]

$$\text{rank}[\Gamma] = \text{rank}[\Gamma|\mathbf{D}]. \tag{17}$$

Due to this invariance condition, there exist $m \times r$ matrix $\mathbf{G}$ such that

$$\mathbf{D} = \Gamma\mathbf{G}. \tag{18}$$

As system (13) is controllable, system (15) is also generically controllable. Consider that system (15) possesses three-time-scale property, so that it can be represented as

$$\begin{bmatrix}\mathbf{z}_{1,k+1}\\ \mathbf{z}_{2,k+1}\\ \mathbf{z}_{3,k+1}\end{bmatrix} = \begin{bmatrix}\Phi_{11} & \Phi_{12} & \Phi_{13}\\ \Phi_{21} & \Phi_{22} & \Phi_{23}\\ \Phi_{31} & \Phi_{32} & \Phi_{33}\end{bmatrix}\begin{bmatrix}\mathbf{z}_{1,k}\\ \mathbf{z}_{2,k}\\ \mathbf{z}_{3,k}\end{bmatrix} + \begin{bmatrix}\Gamma_1\\ \Gamma_2\\ \Gamma_3\end{bmatrix}\mathbf{u}_k + \begin{bmatrix}\mathbf{D}_1\\ \mathbf{D}_2\\ \mathbf{D}_3\end{bmatrix}\mathbf{f}_k \tag{19}$$

$$\mathbf{y}_k = [\mathbf{M}_1 \quad \mathbf{M}_2 \quad \mathbf{M}_3]\left[\mathbf{z}_{1,k}^T \quad \mathbf{z}_{2,k}^T \quad \mathbf{z}_{3,k}^T\right]^T \tag{20}$$

where $\mathbf{z}_{1,k} \in \Re^{n_1}$, $\mathbf{z}_{2,k} \in \Re^{n_2}$, and $\mathbf{z}_{3,k} \in \Re^{n_3}$ denote the states such that $n_1+n_2+n_3 = n$ and the matrices Φ_{ij}, Γ_i, $\mathbf{M}_i$, and $\mathbf{D}_i$ are of suitable dimensions. Furthermore, from (18), it is obvious that

$$\mathbf{D}_1 = \Gamma_1\mathbf{G}, \quad \mathbf{D}_2 = \Gamma_2\mathbf{G}, \quad \mathbf{D}_3 = \Gamma_3\mathbf{G}. \tag{21}$$

Now, with (21), system (19) is rearranged as

$$\begin{bmatrix}\mathbf{z}_{1,k+1}\\ \mathbf{z}_{2,k+1}\\ \mathbf{z}_{3,k+1}\end{bmatrix} = \begin{bmatrix}\Phi_{11} & \Phi_{12} & \Phi_{13}\\ \Phi_{21} & \Phi_{22} & \Phi_{23}\\ \Phi_{31} & \Phi_{32} & \Phi_{33}\end{bmatrix}\begin{bmatrix}\mathbf{z}_{1,k}\\ \mathbf{z}_{2,k}\\ \mathbf{z}_{3,k}\end{bmatrix} + \begin{bmatrix}\Gamma_1\\ \Gamma_2\\ \Gamma_3\end{bmatrix}(\mathbf{u}_k + \mathbf{G}\mathbf{f}_k). \tag{22}$$

System (22) can be decoupled into three subsystems and represented in block diagonal form [8], [9], [30] as

$$\begin{bmatrix}\mathbf{z}_{s,k+1}\\ \mathbf{z}_{f1,k+1}\\ \mathbf{z}_{f2,k+1}\end{bmatrix} = \begin{bmatrix}\Phi_s & \mathbf{0} & \mathbf{0}\\ \mathbf{0} & \Phi_{f1} & \mathbf{0}\\ \mathbf{0} & \mathbf{0} & \Phi_{f2}\end{bmatrix}\begin{bmatrix}\mathbf{z}_{s,k}\\ \mathbf{z}_{f1,k}\\ \mathbf{z}_{f2,k}\end{bmatrix} + \begin{bmatrix}\Gamma_s\\ \Gamma_{f1}\\ \Gamma_{f2}\end{bmatrix}(\mathbf{u}_k + \mathbf{G}\mathbf{f}_k) \tag{23}$$

where $\mathbf{z}_{s,k} \in \Re^{n_1}$, $\mathbf{z}_{f1,k} \in \Re^{n_2}$, and $\mathbf{z}_{f2,k} \in \Re^{n_3}$ denote, respectively, slow, fast 1, and fast 2 states. The relation between the states of (22) and the states of (23) is given by

$$\mathbf{z}_{d,k} = \mathbf{T}\mathbf{z}_k \tag{24}$$

where $\mathbf{z}_{d,k} = [\mathbf{z}_{s,k}^T \ \mathbf{z}_{f1,k}^T \ \mathbf{z}_{f2,k}^T]^T$, $\mathbf{z}_k = [\mathbf{z}_{1,k}^T \ \mathbf{z}_{2,k}^T \ \mathbf{z}_{3,k}^T]^T$, and the transformation matrix $\mathbf{T} \in \Re^{n\times n}$. Since system (19) is assumed to be controllable, pairs (Φ_s, Γ_s), (Φ_{f1}, Γ_{f1}), and (Φ_{f2}, Γ_{f2}) are also controllable [9]. Now, it is assumed that fast 1 and fast 2 subsystems are stable. This assumption is required for two reasons. First, in the case of majority of physical systems, fast modes are stable. If fast modes are not stable, then one has to design controls for all the subsystems to obtain composite control satisfying full-order system, which increase the design complexity. Moreover, the problem of nuclear reactor considered in this brief has stable fast 1 and fast 2 modes. Second, although original singularly perturbed system (19) can be decoupled into three lower order subsystems, a similar kind of decomposition does not hold for control law and disturbance. The control law and disturbance can only be decomposed in time scales but not in dimensions. Therefore, when it comes to disturbance rejection, one can only have one subsystem that enters the sliding mode unless an appropriate dimensional decomposition in the control law is achieved [10]. Hence, DSMC is designed, for system (19) using slow subsystem alone. For that, from (23), slow subsystem can be written as

$$\mathbf{z}_{s,k+1} = \Phi_s\mathbf{z}_{s,k} + \Gamma_s(\mathbf{u}_k + \mathbf{G}\mathbf{f}_k). \tag{25}$$

The relationship between slow subsystem states (25) and states of system (23) is given by

$$\mathbf{z}_{s,k} = [\mathbf{E}_{n_1} \quad \mathbf{0} \quad \mathbf{0}]\mathbf{z}_{d,k} = \mathbf{T}_s\mathbf{z}_{d,k} \tag{26}$$

where $\mathbf{E}_{n_1}$ is the identity matrix of order n_1. If $1 \le m \le n_1$ and $\text{rank}(\Gamma_s) = m$, there exits an orthogonal transformation matrix $\bar{\mathbf{T}} \in \Re^{n_1\times n_1}$ for system (25) such that $\bar{\mathbf{T}}\Gamma_s = [\mathbf{0} \ \bar{\Gamma}_{s2}^T]^T$,

where $\bar{\Gamma}_{s2} \in \Re^{m\times m}$ and is nonsingular. Under this transformation, system (25) is transformed into regular form [2] as

$$\bar{\mathbf{z}}_{s,k+1} = \begin{bmatrix} \bar{\Phi}_{s11} & \bar{\Phi}_{s12} \\ \bar{\Phi}_{s21} & \bar{\Phi}_{s22} \end{bmatrix} \bar{\mathbf{z}}_{s,k} + \begin{bmatrix} \mathbf{0} \\ \bar{\Gamma}_{s2} \end{bmatrix} (\mathbf{u}_k + \mathbf{G}\mathbf{f}_k) \quad (27)$$

such that $\bar{\mathbf{z}}_{s,k} = \bar{\mathbf{T}}\mathbf{z}_{s,k}$, where $\bar{\mathbf{z}}_{s,k} = [\bar{\mathbf{z}}_{s1,k}^T \ \bar{\mathbf{z}}_{s2,k}^T]^T$ with $\bar{\mathbf{z}}_{s1,k} \in \Re^{n_1-m}$ and $\bar{\mathbf{z}}_{s2,k} \in \Re^m$.

A. Design of Sliding Surface

Let us define a sliding function [2] for (27) as $\mathbf{s}_{s,k} = \bar{\mathbf{c}}^T\bar{\mathbf{z}}_{s,k}$ with parameter as

$$\bar{\mathbf{c}}^T = [\mathbf{K} \quad \mathbf{E}_m] \quad (28)$$

where $\mathbf{K}$ is $m \times (n_1 - m)$ matrix. Now

$$\mathbf{s}_{s,k} = \bar{\mathbf{c}}^T\bar{\mathbf{z}}_{s,k} = 0. \quad (29)$$

Hence, from (28) and (29), one can easily find the relationship

$$\bar{\mathbf{z}}_{s2,k} = -\mathbf{K}\bar{\mathbf{z}}_{s1,k}. \quad (30)$$

Then, the sliding mode dynamics of $\bar{\mathbf{z}}_{s1,k}$ can be represented as

$$\bar{\mathbf{z}}_{s1,k+1} = (\bar{\Phi}_{s11} - \bar{\Phi}_{s12}\mathbf{K})\bar{\mathbf{z}}_{s1,k}. \quad (31)$$

If $\mathbf{K}$ is so designed that the eigenvalues of $(\bar{\Phi}_{s11} - \bar{\Phi}_{s12}\mathbf{K})$ are assigned within the unit circle, then $\bar{\mathbf{z}}_{s1,k}$ is stabilized during sliding phase. Consequently, from (30), $\bar{\mathbf{z}}_{s2,k}$ is also stable confined to the sliding surface. Thus, the stability requirement of the sliding surface is achieved. Now, the sliding surface for system (25) can be expressed in terms of the original states as

$$\mathbf{s}_{s,k} = \bar{\mathbf{c}}^T\bar{\mathbf{z}}_{s,k} = \bar{\mathbf{c}}^T\bar{\mathbf{T}}\mathbf{z}_{s,k} = \mathbf{c}^T\mathbf{z}_{s,k}. \quad (32)$$

Lemma 1: If motion around $\mathbf{s}_{s,k} = \mathbf{c}^T\mathbf{z}_{s,k}$, for system (25) is stable, then the motion around

$$\mathbf{s}_k = \mathbf{c}^T\mathbf{T}_s\mathbf{T}\mathbf{z}_k \quad (33)$$

for system (15) is also stable.

Proof 1: Refer to the Appendix.

B. Design of Discrete-Time Sliding Mode Control

Once a sliding surface is designed, DSMC can be obtained using the reaching law approach. From [31], the reaching law for slow subsystem (25) is obtained as

$$\mathbf{s}_{s,k+1} - \mathbf{s}_{s,k} = -q\tau\mathbf{s}_{s,k} - \epsilon\tau\,\mathrm{sgn}(\mathbf{s}_{s,k}) \quad (34)$$

where $\tau > 0$ is a sampling interval, $\epsilon > 0$, $q > 0$, $(1 - q\tau) > 0$. Discrete-time controller for system (25) using stable sliding surface (32) can be obtained from (34) as

$$\mathbf{u}_k = -(\mathbf{c}^T\Gamma_s)^{-1}\big[\mathbf{c}^T\Phi_s\mathbf{z}_{s,k} + q\tau\mathbf{c}^T\mathbf{z}_{s,k} - \mathbf{s}_{s,k} + \epsilon\tau\,\mathrm{sgn}(\mathbf{s}_{s,k})\big] - \mathbf{G}\mathbf{f}_k \quad (35)$$

where $\mathrm{sgn}(\cdot)$ is signum function. In (35), $\mathbf{G}\mathbf{f}_k$ is generally unknown, so the control in this form cannot be implemented and the invariance property of the sliding mode is not yet achievable. To solve this problem, $\mathbf{G}\mathbf{f}_k$ is replaced by $\tilde{\mathbf{G}}_k$ of the same dimensions, which must be sufficiently conservative to maintain the discrete reaching condition. Then, (35) becomes

$$\mathbf{u}_k = -(\mathbf{c}^T\Gamma_s)^{-1}\big[\mathbf{c}^T\Phi_s\mathbf{z}_{s,k} + q\tau\mathbf{c}^T\mathbf{z}_{s,k} - \mathbf{s}_{s,k} + \epsilon\tau\,\mathrm{sgn}(\mathbf{s}_{s,k})\big] - \tilde{\mathbf{G}}_k. \quad (36)$$

The selection of $\tilde{\mathbf{G}}_k$ will be done in a way similar to that developed in [16]. Using (25), (32), and (36), the incremental change in $\mathbf{s}_{s,k}$ can be expressed as

$$\mathbf{s}_{s,k+1} - \mathbf{s}_{s,k} = -q\tau\mathbf{c}^T\mathbf{z}_{s,k} - \epsilon\tau\,\mathrm{sgn}(\mathbf{s}_{s,k}) - \tilde{\mathbf{Y}}_k + \mathbf{Y}_k. \quad (37)$$

where $\tilde{\mathbf{Y}}_k = \mathbf{c}^T\Gamma_s\tilde{\mathbf{G}}_k$ and $\mathbf{Y}_k = \mathbf{c}^T\Gamma_s\mathbf{G}\mathbf{f}_k$. It is reasonable to assume that the bounds of $\mathbf{Y}_k$ are known as $\mathbf{Y}_l \le \mathbf{Y} \le \mathbf{Y}_u$, where $\mathbf{Y}_l$ and $\mathbf{Y}_u$ are, respectively, the upper and lower bounds of the external disturbance. The choice of $\tilde{\mathbf{Y}}_k$ should ensure that the deviation of trajectory from the sliding surface is minimum. The mean and spread of $\mathbf{Y}_k$ can be defined as $\mathbf{Y}_0 = (\mathbf{Y}_l + \mathbf{Y}_u)/2$ and $\mathbf{Y}_1 = (\mathbf{Y}_u - \mathbf{Y}_l)/2$, respectively. Hence, the reaching law can be given by

$$\mathbf{s}_{s,k+1} - \mathbf{s}_{s,k} = -q\tau\mathbf{c}^T\mathbf{z}_{s,k} - (\mathbf{Y}_1 + \epsilon\tau)\mathrm{sgn}(\mathbf{s}_{s,k}) - \mathbf{Y}_0 + \mathbf{Y}_k. \quad (38)$$

The control law (36) is then conveniently put in the form

$$\mathbf{u}_k = \mathbf{F}\mathbf{z}_{s,k} + \vartheta + p\cdot\mathrm{sgn}(\mathbf{s}_{s,k}) \quad (39)$$

where $\mathbf{F} = -(\mathbf{c}^T\Gamma_s)^{-1}\mathbf{c}^T(\Phi_s - \mathbf{E}_{n1} + q\tau)$, $\vartheta = -(\mathbf{c}^T\Gamma_s)^{-1}\mathbf{Y}_0$ and $p = -(\mathbf{c}^T\Gamma_s)^{-1}(\mathbf{Y}_1 + \epsilon\tau)$. This control will bring quasi-sliding mode motion for system (25).

Lemma 2: If the control (39) is expressed in terms of the states of the original system (19) as

$$\mathbf{u}_k = \mathbf{F}\mathbf{T}_s\mathbf{T}\mathbf{z}_k + \vartheta + p\cdot\mathrm{sgn}(\mathbf{c}^T\mathbf{T}_s\mathbf{T}\mathbf{z}_k) \quad (40)$$

and applied to the same, it results in a quasi-sliding mode motion of (19).

Proof 2: Refer to the Appendix.

V. Application to AHWR

A. Controller Design

In general, small and medium size nuclear reactors can be effectively controlled by feedback of global power alone. However, large nuclear reactor, like AHWR, requires feedback of spatial power distribution along with the global power feedback for efficient control. Therefore, the control input, $\mathbf{u}$ in (11), is given by

$$\mathbf{u} = \mathbf{u}_{\mathrm{gp}} + \mathbf{u}_{\mathrm{sp}} \quad (41)$$

where $\mathbf{u}_{\mathrm{gp}}$ is the global power component, designed in [21], and $\mathbf{u}_{\mathrm{sp}}$ is the spatial power component. After the application of (41) to system (11), one can obtain

$$\dot{\mathbf{z}} = \hat{\mathbf{A}}\mathbf{z} + \mathbf{B}\mathbf{u}_{\mathrm{sp}} + \mathbf{B}_f\delta q_f \quad (42)$$

where $\hat{\mathbf{A}}$ is the closed-loop system matrix with global power feedback [21]. System (42) is observed to be controllable. This system also has eigenvalues falling in three distinct clusters: 1) cluster of 38 eigenvalues ranging from 6.2899×10^{-3} to $(8.8268 \pm j1.8656) \times 10^{-5}$; 2) cluster of 35 eigenvalues

that ranges from -1.8396×10^{-1} to -1.1779×10^{-2}; and 3) cluster of 17 eigenvalues ranging from -2.7626×10^{2} to -7.2513 as slow, fast 1, and fast 2 subsystems, respectively. It is worth noting that, despite the application of global power feedback, the closed-loop system possesses four eigenvalues with positive real parts and three eigenvalues at the origin. These unstable eigenvalues are in slow subsystem. However, no considerable change in the locations of eigenvalues of fast 1 and fast 2 subsystems is observed, i.e., they remain stable. Hence, in addition to global power feedback, spatial power feedback is also required.

For properly selected sampling time, discrete version of the continuous-time system, exhibiting three-time-scale property, also exhibits three-time-scale property [25]. In the case of AHWR, selection of sampling interval is based on time constant of delayed neutron precursor, which is of the order of 159 s [26]. Since the reactor power can undergo large variations in small time, it is desirable to have small sampling time from practical implementation point of view and also at the same time system should possess three-time-scale property from design point of view. For the several values of sampling period above 2 s, the proposed controller gives stable response but gain magnitude increases. However, below 2 s, time-scale property is violated. Hence, τ is selected as 2 s and system (42) is discretized to obtain

$$\mathbf{z}_{k+1} = \Phi \mathbf{z}_k + \Gamma \mathbf{u}_k \tag{43}$$

where $\Phi = e^{\hat{\mathbf{A}}\tau}$ and $\Gamma = \int_0^\tau e^{\hat{\mathbf{A}}s}\mathbf{B}ds$. In (42), $\mathbf{u}_{\text{gp}}$ is applied on continuous basis, i.e., on finer time steps for controlling fast transients in the global power. Also recall that, q_f is proportional to global power, hence q_f is also applied on continuous basis. Therefore, system (42) is discretized without feed flow rate input. Moreover, rank$[\mathbf{B}] \neq$ rank$[\mathbf{B}|\mathbf{B}_f]$. Hence, matching condition cannot be satisfied. However, this can be achieved by taking $\mathbf{B} = \mathbf{D}_c$, given in (13) [30]. As a result, discrete system (43) is rewritten as

$$\mathbf{z}_{k+1} = \Phi \mathbf{z}_k + \Gamma \mathbf{u}_k + \mathbf{D}\mathbf{f}_k \tag{44}$$

where $\Gamma = \mathbf{D}$. Now, the discrete-time model (44) is block diagonalized into a slow subsystem of order 38, fast 1 subsystem of order 35, and fast 2 subsystem of order 17, with the state vector (8), partitioned as

$$\begin{aligned} \mathbf{z}_{1,k} &= \begin{bmatrix} \mathbf{z}_H^T & \mathbf{z}_X^T & \mathbf{z}_I^T \end{bmatrix}^T \\ \mathbf{z}_{2,k} &= \begin{bmatrix} \delta h_d & \mathbf{z}_C^T & \mathbf{z}_x^T \end{bmatrix}^T \\ \mathbf{z}_{3,k} &= \mathbf{z}_P. \end{aligned} \tag{45}$$

The matrices Φ, Γ, and $\mathbf{M}$ are partitioned accordingly and decoupled subsystem matrices are determined. It is observed that the eigenvalues of the slow, fast 1, and fast 2 subsystems are in agreement with the largest 38, intermediate 35, and the smallest 17 eigenvalues of the original system. It is also verified that the slow, fast 1, and fast 2 subsystems are controllable and rank$(\Gamma_s) = m$. Furthermore, it is verified that the eigenvalues of fast 1 and fast 2 subsystems are stable, i.e., within unit circle in z-plane. Hence, DSMC is designed simply for the slow subsystem.

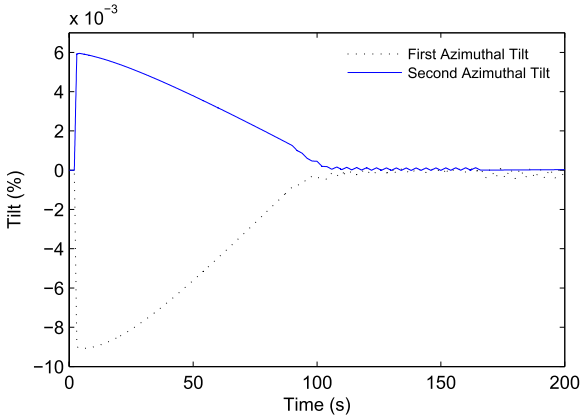

Fig. 1. Variations in azimuthal tilts.

The stable sliding surface for slow subsystem is determined using the procedure given in Section IV-A. With the hyperplane matrix $\mathbf{c}^T$ of order (4×38), sliding surface for original system of AHWR is formulated satisfying (33). After that, the overall DSMC law is constructed. All the 90 eigenvalues of AHWR system are found to be stable. Since sampling time τ is 2 s, q is selected as 0.05, so that the condition $(1 - q\tau) > 0$ is satisfied. Furthermore, ϵ is taken as 0.005. Thus, the width of quasi-sliding mode band is found to be $\delta \leq 0.0026$. Using all these parameters, $\mathbf{F}$ of order (4×38) is calculated and the control (40) is formulated.

B. Transient Simulations

The response of the closed-loop system with the proposed DSMC has been evaluated by carrying out simulations using vectorized nonlinear model [22] of AHWR obtained from set of equations (1)–(7). In addition, these nonlinear simulation results are compared with CSMC [28] and DSMC both obtained by two-stage decomposition, under the same representative transients. This two-stage DSMC is the discrete-time version of CSMC [28] with reaching condition (34), whereas in the case of CSMC sigmoid function is used [28]. Performances of these control techniques are examined with three different transient conditions.

First consider the disturbance in the RR position as the case of state regulation. The system is assumed to be operating at steady state, with all RRs at their equilibrium positions (i.e., 66.07% in). Now by giving proper control signal, quickly RR2, originally under auto control was driven out by almost 1% manually, and left under the effect of automatic control thereafter. This initiated the perturbations in spatial and global power distribution, which were suppressed by the proposed controller, as shown in Figs. 1 and 2. Spatial oscillations are measured in terms of first and second azimuthal tilts [28], as shown in Fig. 1. Since the disturbance is of very short duration, spatial power variations are observed to be very small and completely suppressed after about 100 s. Global power variations obtained with all the controllers, during the transient, are shown in Fig. 2. From the zoomed-in part of Fig. 2, it can be noted that, the performances of both the proposed DSMC and two-stage DSMC, are nearly same and

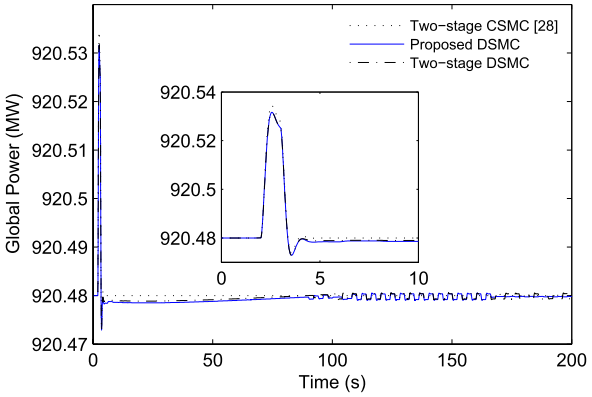

Fig. 2. Comparison of global power variations.

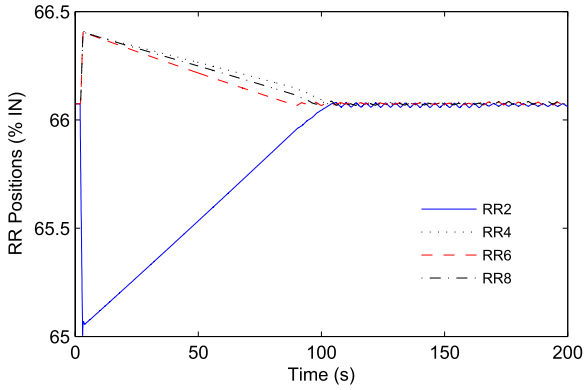

Fig. 3. Variations in RR positions.

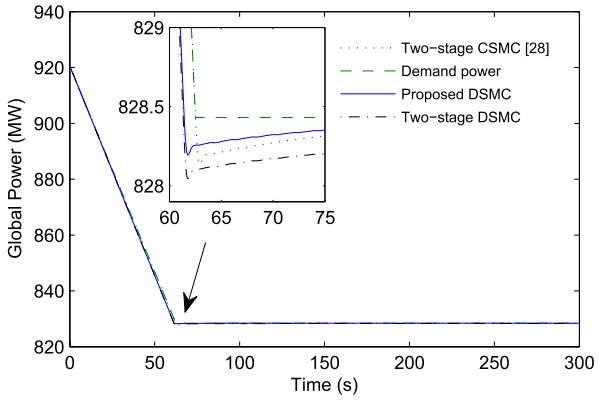

Fig. 4. Global power variations during power maneuvering from 920.48 to 828.43 MW.

slightly better than CSMC. When RR2 is driven out by 1%, all other RRs are driven in and come back to their equilibrium position of 66.07% within about 100 s, as presented in Fig. 3.

In the second transient, power maneuvering is considered. In this demand in global power is decreased uniformly, from steady-state value of 920.48–828.43 MW at the rate of 1.5 MW/s in approximately 61 s and maintained constant thereafter. This transient can be considered as the case of trajectory tracking. During the transient, variations in global power obtained with different controllers are shown in Fig. 4. Although in all the controls, global power is following the

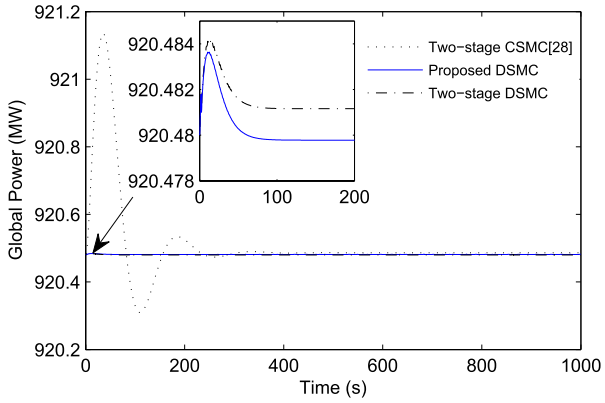

Fig. 5. Global power variations due to positive step change of 5% in feed flow.

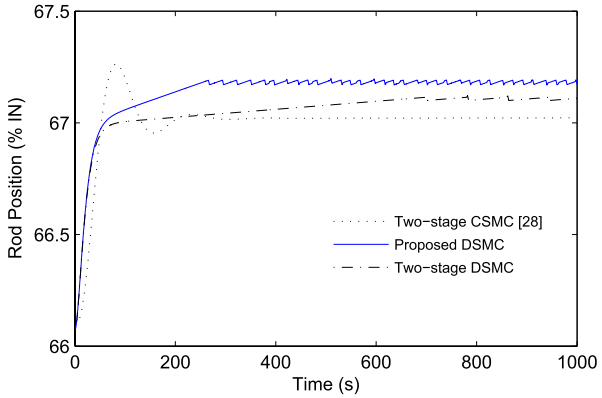

Fig. 6. Variations in RRs positions due to positive step change of 5% in feed flow.

demand power exactly, response of the suggested controller is found to be superior to other controllers. This can be evident from the zoomed-in part of Fig. 4. However, in all the controllers, after attaining demand power, no variations were observed during a long-term simulation.

Furthermore, the response of the system is assessed by giving disturbance in feed water flow and transient is simulated with nonlinear model of AHWR. For this disturbance, positive step change of 5% was introduced in feed flow, when the reactor was operating at steady state. As a result of this, the global power underwent variations, as given in Fig. 5. Due to the controller action, global as well as nodal powers are regulated at their respective steady-state values. This is compensated by changing the position of RRs, as shown in Fig. 6. From Fig. 5, it can be observed that the proposed controller and two-stage DSMC are completely insensitive to the disturbance in the feed flow, whereas, global power variations with CSMC are about 0.076%. Further zooming the portion of global power variations, it is observed that there exists some steady-state error with two-stage DSMC. Again from Fig. 6, it can be observed that RRs take almost 800 s to settle to the new steady state with two-stage DSMC compared with 270 s taken by the proposed DSMC.

From the transient simulations, it can be noted that the performance of DSMCs, both the proposed and two-stage, is better than CSMC as far as regulation, tracking, and disturbance rejection are concerned. However, the close observation

of the proposed and the two-stage DSMC shows that the proposed controller is performing well. Moreover, it is observed that the gain magnitude obtained with the two-stage DSMC is near about three to four times greater than that of the proposed one. This is because of the combination of slow and fast 1 modes to form slow subsystem in two-stage decomposition. Hence, the overall performance of the proposed DSMC is better than other controllers.

VI. Conclusion

In this brief, the design of DSMC for matched uncertain three-time-system is presented. The suggested method is then explored for spatial power stabilization of AHWR. The AHWR system is linearized and is decomposed into three subsystems by direct block diagonalization. DSMC law is then designed using only the slow subsystem states. Subsequently, the DSMC law for full-order system is obtained. Effectiveness of the proposed controller is established from the simulations carried out under different transient conditions with vectorized nonlinear model. Furthermore, the results obtained with the suggested controller are compared with the other sliding mode controllers and the performance is found to be superior.

Appendix

Proof 1: As $\mathbf{s}_{s,k} = \mathbf{c}^T\mathbf{z}_{s,k}$ is a stable sliding surface for (25), the motion around $\mathbf{s}_{s,k}$ can be obtained by setting $\mathbf{s}_{s,k+1} = 0$. Therefore, the equivalent DSMC law is

$$\mathbf{u}_k = -(\mathbf{c}^T\Gamma_s)^{-1}\mathbf{c}^T\Phi_s\mathbf{z}_{s,k} - \mathbf{G}\mathbf{f}_k. \tag{46}$$

Thus, the motion along $\mathbf{z}_{s,k}$ is given by

$$\mathbf{z}_{s,k+1} = (\Phi_s - \Gamma_s(\mathbf{c}^T\Gamma_s)^{-1}\mathbf{c}^T\Phi_s)\mathbf{z}_{s,k}. \tag{47}$$

As (47) is stable by design, eigenvalues of $(\Phi_s - \Gamma_s(\mathbf{c}^T\Gamma_s)^{-1}\mathbf{c}^T\Phi_s)$ will be stable. Now, the motion around $\mathbf{s}_k = \mathbf{c}^T\mathbf{T}_s\mathbf{z}_{d,k}$ for system (23) is obtained by setting $\mathbf{s}_{k+1} = 0$ and writing

$$\mathbf{u}_k = -(\mathbf{c}^T\Gamma_s)^{-1}\mathbf{c}^T[\Phi_s \quad \mathbf{0} \quad \mathbf{0}]\mathbf{z}_{d,k} - \mathbf{G}\mathbf{f}_k. \tag{48}$$

Hence, the motion around the switching surface $\mathbf{s}_k$ is

$$\mathbf{z}_{d,k+1} = \begin{bmatrix} \Phi_s - \Gamma_s(\mathbf{c}^T\Gamma_s)^{-1}\mathbf{c}^T\Phi_s & \mathbf{0} & \mathbf{0} \\ -\Gamma_{f1}(\mathbf{c}^T\Gamma_s)^{-1}\mathbf{c}^T\Phi_s & \Phi_{f1} & \mathbf{0} \\ -\Gamma_{f2}(\mathbf{c}^T\Gamma_s)^{-1}\mathbf{c}^T\Phi_s & \mathbf{0} & \Phi_{f2} \end{bmatrix}\mathbf{z}_{d,k}. \tag{49}$$

As $(\Phi_s - \Gamma_s(\mathbf{c}^T\Gamma_s)^{-1}\mathbf{c}^T\Phi_s)$ is stable by design and Φ_{f1} and Φ_{f2} are assumed to be stable, the sliding motion of $\mathbf{s}_k = \mathbf{c}^T\mathbf{T}_s\mathbf{z}_{d,k}$ is stable. Furthermore, systems (19) and (23) are related through (24), therefore (33) is stable sliding surface for (19) and consequently for system (15).

Proof 2: If it can be shown that the control law

$$\mathbf{u}_k = \mathbf{F}\mathbf{T}_s\mathbf{z}_{d,k} + \vartheta + p\cdot\mathrm{sgn}(\mathbf{c}^T\mathbf{T}_s\mathbf{z}_{d,k}) \tag{50}$$

is able to bring a sliding mode motion for system (23), then

$$\mathbf{u}_k = \mathbf{F}\mathbf{T}_s\mathbf{T}\mathbf{z}_k + \vartheta + p\cdot\mathrm{sgn}(\mathbf{c}^T\mathbf{T}_s\mathbf{T}\mathbf{z}_k) \tag{51}$$

will bring a sliding mode motion for system (19). Therefore, from (32), the reaching law (38) can be expressed as

$$\begin{aligned}&\mathbf{c}^T\mathbf{z}_{s,k+1} - \mathbf{c}^T\mathbf{z}_{s,k}\\ &\quad = -q\tau\mathbf{c}^T\mathbf{z}_{s,k} - (\mathbf{Y}_1 + \epsilon\tau)\mathrm{sgn}(\mathbf{c}^T\mathbf{z}_{s,k}) - \mathbf{Y}_0 + \mathbf{Y}_k.\end{aligned} \tag{52}$$

Using relations (24) and (26), the reaching law (52) can be rewritten as

$$\begin{aligned}&\mathbf{c}^T\mathbf{T}_s\mathbf{T}\mathbf{z}_{k+1} - \mathbf{c}^T\mathbf{T}_s\mathbf{T}\mathbf{z}_k\\ &= -q\tau\mathbf{c}^T\mathbf{T}_s\mathbf{T}\mathbf{z}_k - (\mathbf{Y}_1 + \epsilon\tau)\mathrm{sgn}(\mathbf{c}^T\mathbf{T}_s\mathbf{T}\mathbf{z}_k) - \mathbf{Y}_0 + \mathbf{Y}_k.\end{aligned} \tag{53}$$

Further using (33), system (53) can be modified to obtain

$$\mathbf{s}_{k+1} - \mathbf{s}_k = -q\tau\mathbf{s}_k - (\mathbf{Y}_1 + \epsilon\tau)\mathrm{sgn}(\mathbf{s}_k) - \mathbf{Y}_0 + \mathbf{Y}_k. \tag{54}$$

Thus, the reaching law (34) is equivalent to the reaching law (54). Therefore, it can be concluded that, any control that satisfies the reaching law (52) [i.e., the reaching law (34)], would automatically satisfy the original system reaching law (54).

Acknowledgment

The authors would like to thank the anonymous reviewers for constructive comments and suggestions to improve the quality of this brief.

References

[1] J. Y. Hung, W. Gao, and J. C. Hung, "Variable structure control: A survey," *IEEE Trans. Ind. Electron.*, vol. 40, no. 1, pp. 2–22, Feb. 1993.

[2] C. Edwards and S. K. Spurgeon, *Sliding Mode Control: Theory and Applications*. Bristol, PA, USA: Taylor & Francis, 1998.

[3] K. D. Young, V. I. Utkin, and U. Ozguner, "A control engineer's guide to sliding mode control," *IEEE Trans. Control Syst. Technol.*, vol. 7, no. 3, pp. 328–342, May 1999.

[4] K. Furuta and Y. Pan, "Variable structure control with sliding sector," *Automatica*, vol. 36, no. 2, pp. 211–228, Feb. 2000.

[5] M. S. Mahmoud, "Algorithms for discrete systems with multi-time scales," in *Control and Dynamic Systems*, vol. 3, C. T. Leonides, Ed. London, U.K.: Academic, 1989, pp. 217–242.

[6] R. G. Phillips, "Reduced order modelling and control of two-time-scale discrete systems," *Int. J. Control*, vol. 31, no. 4, pp. 765–780, 1980.

[7] M. S. Mahmoud, "Order reduction and control of discrete systems," *IEE Proc. D, Control Theory Appl.*, vol. 129, no. 4, pp. 129–135, Jul. 1982.

[8] D. S. Naidu, *Singular Perturbation Methodology in Control System*. London, U.K.: Peregrinus, 1988.

[9] S. R. Shimjith, A. P. Tiwari, and B. Bandyopadhyay, "Design of fast output sampling controller for three-time-scale systems: Application to spatial control of advanced heavy water reactor," *IEEE Trans. Nucl. Sci.*, vol. 58, no. 6, pp. 3305–3316, Dec. 2011.

[10] T. S. Li, J.-L. Lin, and F.-C. Kung, "Design of sliding-mode controller for discrete singular perturbation systems," in *Proc. IEEE 21st Int. Conf. Ind. Electron., Control, Instrum.*, Nov. 1995, pp. 736–741.

[11] B. Bandyopadhyay, A. G'Egziabher Abera, and S. Janardhanan, "Sliding mode control design via reduced order model approach," in *Proc. IEEE Int. Conf. Ind. Technol.*, Dec. 2006, pp. 1538–1541.

[12] G. D. Reddy, B. Bandyopadhyay, and A. P. Tiwari, "Discrete-time sliding mode control for two-time-scale systems," in *Proc. 34th IEEE Int. Conf. Ind. Electron.*, Nov. 2008, pp. 170–175.

[13] T. Nguyen, W.-C. Su, and Z. Gajic, "Singular perturbation analysis of discrete-time output feedback sliding mode control with disturbance attenuation," in *Proc. Amer. Control Conf.*, Jun. 2009, pp. 757–762.

[14] R. K. Sinha and A. Kakodkar, "Design and development of the AHWR—The Indian thorium fuelled innovative nuclear reactor," *Nucl. Eng. Design*, vol. 236, nos. 7–8, pp. 683–700, Apr. 2006.

[15] G. D. Reddy, Y. Park, B. Bandyopadhyay, and A. P. Tiwari, "Discrete-time output feedback sliding mode control for spatial control of a large PHWR," *Automatica*, vol. 45, no. 9, pp. 2159–2163, Sep. 2009.

[16] G. D. Reddy, B. Bandyopadhyay, and A. P. Tiwari, "Multirate output feedback based sliding mode spatial control for a large PHWR," *IEEE Trans. Nucl. Sci.*, vol. 54, no. 6, pp. 2677–2686, Dec. 2007.

[17] J. J. Duderstadt and L. J. Hamilton, *Nuclear Reactor Analysis*. New York, NY, USA: Wiley, Jan. 1976.

[18] S. R. Shimjith, A. P. Tiwari, M. Naskar, and B. Bandyopadhyay, "Space–time kinetics modeling of advanced heavy water reactor for control studies," *Ann. Nucl. Energy*, vol. 37, no. 3, pp. 310–324, Mar. 2010.

[19] S. R. Shimjith, A. P. Tiwari, and B. Bandyopadhyay, "Coupled neutronics-thermal hydraulics model of advanced heavy water reactor for control system studies," in *Proc. IEEE Int. Conf. INDICON*, Kanpur, India, Dec. 2008, pp. 126–131.

[20] K. J. Astrom and R. D. Bell, "Drum-boiler dynamics," *Automatica*, vol. 36, no. 3, pp. 363–378, Mar. 2000.

[21] S. R. Shimjith, A. P. Tiwari, B. Bandyopadhyay, and R. K. Patil, "Spatial stabilization of advanced heavy water reactor," *Ann. Nucl. Energy*, vol. 38, no. 7, pp. 1545–1558, Jul. 2011.

[22] R. K. Munje, B. M. Patre, and A. P. Tiwari, "Non-linear simulation and control of xenon induced oscillations in advanced heavy water reactor," *Ann. Nucl. Energy*, vol. 64, pp. 191–200, Feb. 2014.

[23] S. R. Shimjith, A. P. Tiwari, and B. Bandyopadhyay, "A three-time-scale approach for design of linear state regulator for spatial control of advanced heavy water reactor," *IEEE Trans. Nucl. Sci.*, vol. 58, no. 3, pp. 1264–1276, Jun. 2011.

[24] R. K. Munje, J. G. Parkhe, and B. M. Patre, "Control of xenon oscillations in advanced heavy water reactor via two-stage decomposition," *Ann. Nucl. Energy*, vol. 77, pp. 326–334, Mar. 2015.

[25] R. K. Munje, P. S. Londhe, J. G. Parkhe, B. M. Patre, and A. P. Tiwari, "Spatial control of advanced heavy water reactor by fast output sampling technique," in *Proc. IEEE Int. Conf. Control Appl.*, Aug. 2013, pp. 1212–1217.

[26] R. K. Munje, B. M. Patre, and A. P. Tiwari, "Periodic output feedback for spatial control of AHWR: A three-time-scale approach," *IEEE Trans. Nucl. Sci.*, vol. 61, no. 4, pp. 2373–2382, Aug. 2014.

[27] P. S. Londhe, B. M. Patre, and A. P. Tiwari, "Design of single-input fuzzy logic controller for spatial control of advanced heavy water reactor," *IEEE Trans. Nucl. Sci.*, vol. 61, no. 2, pp. 901–911, Apr. 2014.

[28] R. K. Munje, B. M. Patre, S. R. Shimjith, and A. P. Tiwari, "Sliding mode control for spatial stabilization of advanced heavy water reactor," *IEEE Trans. Nucl. Sci.*, vol. 60, no. 4, pp. 3040–3050, Aug. 2013.

[29] B. Drazenovic, "The invariance conditions in variable structure systems," *Automatica*, vol. 5, no. 3, pp. 287–295, May 1969.

[30] T. Nguyen, W.-C. Su, and Z. Gajic, "Variable structure control for singularly perturbed linear continuous systems with matched disturbances," *IEEE Trans. Autom. Control*, vol. 57, no. 3, pp. 777–783, Mar. 2012.

[31] W. Gao, Y. Wang, and A. Homaifa, "Discrete-time variable structure control systems," *IEEE Trans. Ind. Electron.*, vol. 42, no. 2, pp. 117–122, Apr. 1995.